The International Archives of the Photogrammetry, Remote Sensing and Spatial Information Sciences, Volume XLVIII-4/W17-2025
GeoAdvances 2025 – 10th International Conference on GeoInformation Advances, 29–30 May 2025, Marrakech, Morocco

A Method for Assessing and Predicting Urban Expansion

Davoud Omarzadeh[1], Mehran Alizadeh Pirbasti[*2], Zahra Ghasemizad Gonbad[3], Gavin McArdle[2],Javier BorgeHolthoefer[1]

[1]Internet Interdisciplinary Institut (IN3) Open University of Catalonia, Barcenola, Spain.
[2]School of Computer Science, University College Dublin, Dublin, Ireland.
[3]University of Tabriz, Iran.

Keywords: Urban spatial expansion, Artificial Intelligence, Multi-criteria Decision-making, GIS, Satellite Images, Machine Learning.

Abstract

This study introduces an integrated framework for assessing and predicting urban expansion, illustrated through the case of Urmia, utilizing artificial intelligence (AI), multi-criteria decision-making (MCDM), and GIS. The multi-layer perceptron (MLP) analysis predicted the total built-up area to be 134.29 km², of which 82.32 km² is currently developed, leaving 51.97 km² available for future expansion. The combined application of Support Vector Machine (SVM), Analytic Network Process (ANP), and MLP techniques demonstrated high accuracy in land use mapping and growth predictions, highlighting the effectiveness of machine learning in addressing urban complexities. Key factors such as geology and proximity to roads were identified as significant drivers of urban growth, indicating the need for localized strategies in future research. This methodology can be applied to similar urban contexts, offering a data-driven approach to sustainable urban planning and effective management of rapid urbanization.

1. Introduction

Uncontrolled urban growth and development have become critical global concerns in recent years (Castanho et al., 2022). Researchers project a significant escalation of these issues by 2050 (Malik et al., 2017, Aziz et al., 2015). This rapid urbanization, coupled with industrialization over the past few decades, has made urban sustainability a universal priority (Mangi et al., 2020). As cities expand physically, they are also experiencing a surge in urban populations, leading to a host of challenges, including inadequate public services, traffic congestion, insufficient housing, and high rates of unemployment and health issues (Al-Fugara et al., 2018). To address these challenges, urban planners and policymakers must develop effective strategies to monitor and manage urban characteristics and their changes over time.

In this context, remote sensing techniques have emerged as vital tools for tackling urban development issues. Among these techniques, satellite image classification plays a crucial role in information extraction (Li et al., 2019, Raj et al., 2017). By analyzing land cover patterns, researchers can derive valuable insights about both natural and social processes, enabling them to model various phenomena (Liang, 2008, Alizadeh Pirbasti et al., 2021). However, satellite image analysis presents challenges, primarily due to the vast data volume and the complexity of the channels through which images are acquired (Buddhiraju and Rizvi, 2010). The accuracy and reliability of classification processes significantly impact the quality of insights drawn from satellite data, emphasizing the need for selecting appropriate methods tailored to specific conditions and types of images. This choice is particularly critical in fields such as urban planning and land use management, where decisions based on inaccurate data can have far-reaching consequences.

At the technical level, image classification is essential for addressing land separation and classification challenges (Omkar et al., 2007). Remote sensing techniques can effectively identify changes in land cover over time (Zurqani et al., 2019), and the integration of new image classification methods can enhance the accuracy of results. Machine learning, for instance, represents a promising advancement in this area (Wingate et al., 2016, Sivasubramaniyan and RajaPerumal, 2024). However, various factors complicate land cover classification using satellite imagery, such as seasonal variations, spectral confusion, shadow effects, mixed pixels, scale effects, and image acquisition conditions, as well as human error (Khatami et al., 2016). These factors can hinder the reliability of classification results, underscoring the necessity for robust methods that facilitate accurate mapping of land cover (Rodriguez-Galiano et al., 2012). Furthermore, utilizing temporal images that capture changes over time is vital for effective land cover monitoring and classification. Yet, processing and analyzing the high volume of these temporal images poses significant challenges, as traditional desktop software often lacks the capacity to handle extensive multi-decade time series data efficiently (Hird et al., 2017).

Fortunately, advancements in remote sensing have led to the development of effective methods for identifying different land cover types. One particularly notable approach for multi-temporal processing of satellite images is the use of the Google Earth Engine (GEE) platform, which has gained popularity among remote sensing specialists (Gorelick et al., 2017, M et al., 2023). GEE has been employed in various studies, including forest monitoring (Omarzadeh et al., 2020, Zurqani et al., 2019), urban environment assessment (Cao et al., 2021), and climate analysis (Kodaka et al., 2021). The platform's integration of machine learning tools enhances its capability to process multi-temporal remote sensing data effectively (Waske et al., 2009). In addition to facilitating land use extraction in urban settings, it is essential to conduct comprehensive studies that examine the factors influencing the physical development of urban areas.

To complement previous investigations, the contribution of our research lies in designing a novel pipeline that provides a comprehensive view of urban sprawl analysis, considering various factors. Meanwhile, we apply reliable machine learning tech-

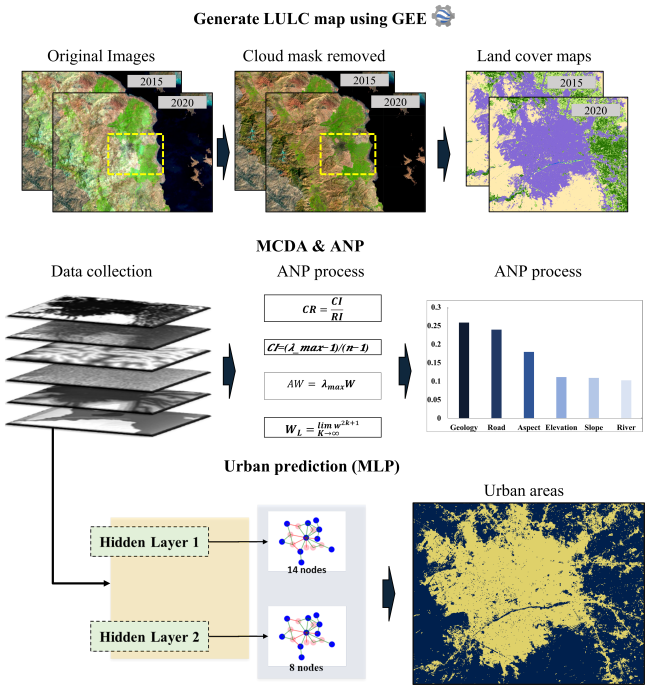

Figure 1. Research Pipeline: The Land Use and Land Cover (LULC) mapping process begins with pre-processing satellite images, which includes spatial masking and cloud removal. Classification is then performed using a Support Vector Machine (SVM) in Google Earth Engine, with training data collected for each year based on corresponding satellite images. The weight values of each criterion are calculated using the Analytic Hierarchy Process (ANP). Finally, a Multi-Layer Perceptron (MLP) model with two hidden layers (14 nodes in the first layer and 8 nodes in the second) is employed to predict potential pixels that will be converted into built-up areas.

niques and utilize cloud-based platforms (such as GEE), to overcome software and hardware limitations in this type of research. On the other hand, an AI approach is applied to integrate geoscience and computer techniques to handle multi-criteria decision analysis to evaluate the urban physical extension.

The present study consists of three main stages. In the first stage, using the capabilities of the GEE platform and machine learning techniques, the land use layer of Urmia for 2015 and 2020 were extracted from Sentinel-2 images. Then, in the second stage, to study urban development, the multi-criteria decision analysis (MCDA) technique and the analytical network process (ANP) method were used to evaluate criteria that drive the growth of the urban physical domain. These criteria include elevation, slope, and aspect, distance from the drainage network derived from the DSM (Tadono et al., 2016), distance from roads collected from Open Street Map, geology sourced from the Natural Resources and Watershed Management Organization of West Azerbaijan, and land use extracted from Sentinel-2 satellite images. These criteria, sourced from various origins, were employed as physical growth drivers in the MCDA to assess and guide urban development. Eventually, in the third stage, an artificial neural network was used to predict the areas appropriate for the development of urban areas, utilizing a multi-layer perceptron (MLP) network. Figure 1 illustrates the pipeline of the research.

2. Study Area

Urmia, located in West Azerbaijan, Iran, was selected for this study due to its rapid urban growth and proximity to the shrinking Urmia Lake, which significantly impacts land use and urban planning. Situated at 37°33´ N and 45°04´ E (see Figure 2), Urmia has undergone substantial demographic and spatial transformations over the decades. In 1956, the city covered an area of 14.44 km² with a population of 164,419. By 1996, the area expanded to 59 km², accommodating 435,200 residents. This growth continued, with the area reaching 112.37 km² and the population increasing to 736,224 by 2016. Recent land use changes have primarily concentrated in urban areas, leading to an expansion of built-up zones. Additionally, the drying of Urmia Lake has created opportunities to repurpose these dried areas for new uses, such as factories, attracting more migrants to the city and contributing to its growth. However, a study by Rostaei highlights significant class disparities and urban spatial inequality, revealing that the distribution of housing conditions among residents is uneven (rostaei et al., 2020), likely a consequence of unplanned urban expansion.

3. Data and Methodology

3.1 Data acquisition

The study used two data types, including Sentinel-2 satellite imagery with 10 meters spatial resolution for 2015 and 2020, and spatial data, which included six criteria. Satellite images were used to extract LULC maps. The LULC layer, coupled with six criteria, was integrated into the MCDA framework for the ANP process implementation. Eventually, these criteria, along with a boolean layer representing the city's physical extent, were introduced as variables in the designed neural network.

The geology layer enabled the identification of rock types and geological stability, which is crucial for assessing terrain suitability. This dataset was obtained from the Geological Survey and Mineral Exploration of Iran at a scale of 1:50,000 and digitized for GIS integration. Elevation, which influences climate, vegetation, and construction potential, was sourced from Global ALOS DSM data (Tadono et al., 2016) and standardized to a 10-meter pixel resolution. Slope, measuring terrain steepness and impacting water runoff, erosion, and construction feasibility, was calculated from Digital Elevation Models (DEMs) using GIS-based slope analysis tools. The slope aspect, determining the direction slopes face and influencing sunlight exposure, vegetation growth, and microclimate, was also derived from DEMs using GIS tools to classify terrain based on compass directions (e.g., north- or south-facing).

Proximity to natural drainage systems, such as rivers and streams, was used to assess flood risk and water availability. Drainage networks were delineated from DEMs through hydrological modeling, and distances were calculated using GIS-based Euclidean distance functions. Similarly, accessibility was evaluated by measuring proximity to road networks, which is essential for urban and infrastructure planning. Road data was sourced from OpenStreetMap, and distances were computed using Euclidean distance functions in GIS. All raster layers used in this study were standardized to a 10-meter pixel resolution, and the criteria employed in the MCDA process were classified into five categories in raster format (Figure 4). Following the extraction of land use data, a boolean map generated by the neural network served as the dependent variable in the analysis.

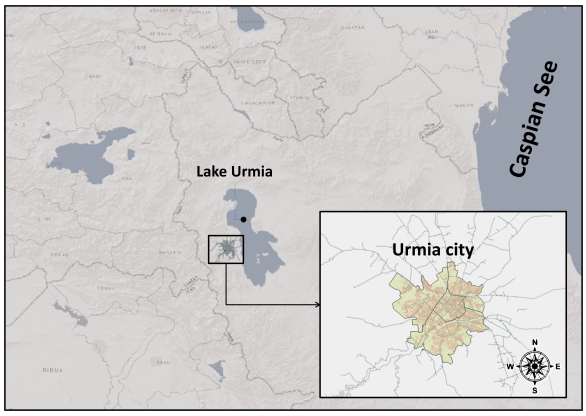

Figure 2. Location of the Study Area

3.2 Methodology

Following the research pipeline, the first stage involved generating an LULC map of the study area using machine learning techniques. Methods like neural networks, random forests, support vector machines, and genetic algorithms are widely used for modeling environmental processes (LeCun et al., 2015, Chen et al., 2021). In this study, Sentinel-2 satellite images were classified using the Google Earth Engine (GEE) platform, which provides access to datasets such as Landsat, Sentinel, and Modis, along with customizable algorithms for image classification and cloud masking (Amani et al., 2019). Specifically, SVM, RF, and MD were tested for classification. Accuracy was assessed using overall accuracy (OA), user accuracy (UA), producer accuracy (PA), and the kappa coefficient, with validation from field-observed data and cadastral data obtained from the Municipality of Urmia City. Based on its superior accuracy, the SVM results were selected for use in the remainder of the research.

The following equations represent the use of each metric in the accuracy assessment task. Where UA represents User Accuracy, PA stands for Producer Accuracy, OA denotes Overall Accuracy, x_{kk} is the sum of correctly classified pixels in both row k and column k for class k, x_{+k} is the total number of predicted instances in column k, x_{k+} represents the total number of predicted instances in row k, and N signifies the total number of pixels. The kappa coefficient, denoted as κ, is calculated with the expected agreement (P_e) as:

$$P_e = \frac{\sum_{i=1}^{k}(A_i \times B_i)}{N^2} \tag{1}$$

Here, k is the number of categories, A_i is the sum of the row totals for category i, B_i is the sum of the column totals for category i, and N is the total number of observations.

$$UA = \left(\frac{x_{kk}}{x_{+k}}\right) \times 100 \tag{2}$$

$$PA = \left(\frac{x_{kk}}{x_{k+}}\right) \times 100 \tag{3}$$

$$OA = \frac{1}{N}\sum_{r=1}^{K} n_i \tag{4}$$

$$\kappa = \frac{OA - P_e}{100 - P_e} \tag{5}$$

In the next stage, the Analytic Network Process (ANP), a Multi-Criteria Decision Analysis (MCDA) method was applied to address complex spatial problems by considering interdependencies among criteria and alternatives (Feizizadeh et al., 2021). ANP is widely used in GIS for site selection, natural resource management, and urban planning (Jamali et al., 2023), offering advantages in incorporating subjective factors and accounting for direct and indirect influences (Alizadeh et al., 2018). To implement ANP, we reviewed existing research in urban studies, GIS, remote sensing, and geology, using pairwise comparisons to evaluate criteria and establish weights for the analysis.

The employed ANP involved the construction of pairwise comparison matrices (6), the calculation of priority vectors, and the formation of supermatrices, as outlined in the method's framework. These matrices were derived using expert judgment and supported by empirical data, comparing the relative importance of each criterion against every other criterion in pairs using a standardized scale introduced by (Saaty, 1996). Typically, a scale of 1 to 9 was used, where 1 indicates equal importance, and 9 represents extreme importance of one criterion over another (Saaty, 1996).

$$A = \begin{pmatrix} 1 & 3 & \frac{1}{2} & 4 & 5 & 2 \\ \frac{1}{3} & 1 & \frac{1}{4} & 3 & 2 & \frac{1}{2} \\ 2 & 4 & 1 & 5 & 3 & 2 \\ \frac{1}{4} & \frac{1}{3} & \frac{1}{5} & 1 & \frac{1}{2} & \frac{1}{3} \\ \frac{1}{5} & \frac{1}{2} & \frac{1}{3} & 2 & 1 & \frac{1}{2} \\ \frac{1}{2} & 2 & \frac{1}{2} & 3 & 2 & 1 \end{pmatrix} \tag{6}$$

The diagonal of the matrix is always 1 since each criterion is equally essential to itself. The next step, after obtaining the pairwise comparison matrix, is the calculation of the priority vector.

$$A\mathbf{w} = \lambda_{\max}\mathbf{w} \tag{7}$$

Where $\mathbf{w}$ represents the matrix multiplication of the pairwise comparison matrix $\mathbf{A}$ and the priority vector $\mathbf{w}$. And $\lambda_{\max}\mathbf{w}$ represents the product of the maximum eigenvalue $\lambda_{\max}$ and the priority vector $\mathbf{w}$. To obtain the final weights of each factor, the supermatrix was operated as the following structure: The supermatrix W is given by:

$$W = \begin{pmatrix} W_{11} & W_{12} & W_{13} & W_{14} & W_{15} & W_{16} \\ W_{21} & W_{22} & W_{23} & W_{24} & W_{25} & W_{26} \\ W_{31} & W_{32} & W_{33} & W_{34} & W_{35} & W_{36} \\ W_{41} & W_{42} & W_{43} & W_{44} & W_{45} & W_{46} \\ W_{51} & W_{52} & W_{53} & W_{54} & W_{55} & W_{56} \\ W_{61} & W_{62} & W_{63} & W_{64} & W_{65} & W_{66} \end{pmatrix} \tag{8}$$

Where each block W_{ij} is defined as:

$$W_{ij} = \begin{pmatrix} w_i \\ w_i \\ w_i \\ w_i \\ w_i \\ w_i \end{pmatrix} \tag{9}$$

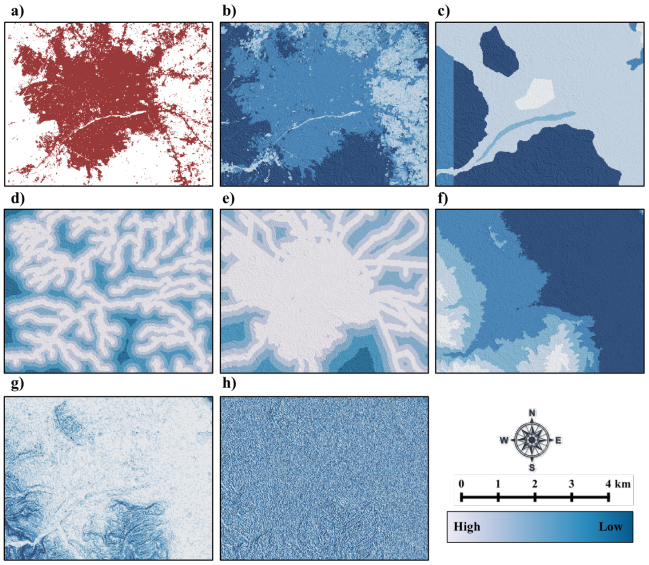

Figure 3. The criteria used in the MCDA to evaluate urban development include: a) the binary layer of built-up areas derived from the LULC map (binary for MLP), b) LULC map, c) Geology, d) Distance to drainage, e) Distance to roads, f) Elevation, g) Slope, and h) Slope aspect. All layers, except for the Boolean one, were standardized, and assigned weights acquired from the ANP process. These weighted layers were then imported into the MLP model, with the Boolean layer serving as the dependent variable and the remaining layers as independent variables, to predict potential built-up areas.

W_{ij} is the block matrix representing the priority vector of criterion i with respect to criterion j. - w_i is the priority vector of the i-th criterion. Diagonal Blocks (W_{ii}): Each diagonal block W_{ii} contains the priority vector for the i-th criterion. These blocks show the relative importance of each criterion with respect to itself, typically reflecting uniform values on the diagonal. Off-Diagonal Blocks (W_{ij} where $i \neq j$): Each off-diagonal block W_{ij} represents the relative importance of criterion i with respect to criterion j. In practice, these would be filled with specific values based on pairwise comparisons, but here, for simplicity, they are shown as containing the priority vector w_i. This block structure allows for the combination of individual priority vectors into a supermatrix, which integrates the different criteria and their relative importance in the decision-making process.

Finally, we use a Multilayer Perceptron (MLP) model to predict potential built-up areas based on land-use/land-cover maps and physical factors (Figure 1). The MLP is trained on LULC data from 2015 to 2020, with six physical layers (elevation, slope aspects, slope, proximity to roads, proximity to rivers, and geology) as input features (Figure 3). The MLP neural network model, commonly referred to as a "backpropagation" network (Ozturk, 2015), is a robust method for performing non-parametric regression analysis. The typical structure of an MLP includes an input layer, one or more hidden layers, and an output layer (Razavi, 2014). The output of the model consists of a neuron map and a predicted membership map, which together represent the forecasted urban expansion based on the defined independent variables (Eastman, 2012).

The MLP operates through two critical phases: forward and backward propagation, which are used to iteratively adjust the connection weights between neurons. For a single node, the

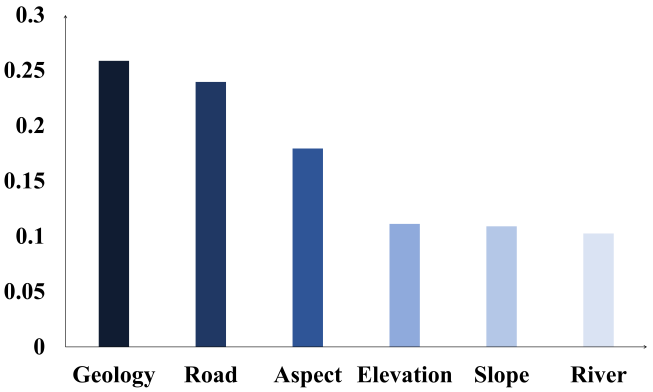

Figure 4. The final weights of the geographical layers influencing urban growth are calculated through the ANP process. The ANP incorporates pairwise comparisons and feedback relationships among criteria to assign these weights. The bar plot identifies Geology and Road as the most influential factors, reflecting their significant role in driving urban expansion relative to other layers (equation 7).

weighted input is computed using Equation 10:

$$\text{net}_j = \sum_{i=1}^{m} W_{ij}\, O_i \tag{10}$$

where W_{ij} represents the weights between nodes i and j, and O_i is the output of node i. The output of the node j is then determined using Equation 11:

$$O_j = f(\text{net}_j) \tag{11}$$

In this study, the activation function f is a sigmoid function, which applies the weights before transmitting signals to the subsequent layer. After the forward pass, the model compares the output nodes with the expected outcomes to compute the error. Our MLP model architecture includes two hidden layers with 14 and 8 nodes, respectively, and uses the ReLU activation function. The model was trained over 1000 iterations, allowing it to effectively capture complex, non-linear relationships between geographical features and land-use changes. To evaluate its predictive capability, the model utilized one dependent variable and eight independent variables. The urban transitions between 2015 and 2020 were designated as the dependent variable, defined in binary terms: if land converted from non-urban to urban within this period, its value was set to Y = 1; otherwise, it was set to Y = 0. The results of these transitions are illustrated in Figure 4 a.

After training, the MLP generates a probability map predicting areas likely to become built up in the future. A boolean layer is applied to constrain the predictions to suitable areas, resulting in a final map that highlights the most probable locations for urban expansion. This approach integrates neural network modeling with GIS data to provide a robust tool for urban growth forecasting.

4. Results

In this study, machine learning techniques were employed to detect and classify Land Use and Land Cover (LULC) changes

for the years 2015 and 2020, focusing on monitoring physical urban expansion through objective and data-driven methods. The analysis utilized exclusively physical data, such as elevation, slope, geology, and satellite-derived LULC changes, without incorporating qualitative factors like population, economics, or policy-based variables. This approach highlights the potential of remote sensing and GIS technologies in urban studies, leveraging consistently available satellite imagery to capture land-use transitions accurately.

The LULC classification process was carried out on the Google Earth Engine (GEE) platform, utilizing three machine learning algorithms: Decision Tree, Support Vector Machine (SVM) and Minimum Distance (MD). A data set comprised 5,150 samples representing five key categories: water, bare land, orchards, cultivated land, and settlements. Of these, 4,000 samples were used for training the models, while 1,150 samples were reserved for testing and validation, ensuring a thorough evaluation of each classifier's performance. Among the tested algorithms, the Support Vector Machine (SVM) demonstrated the highest accuracy, achieving Kappa coefficients of 0.84 for the 2020 classification and 0.82 for the 2015 classification. These results indicate a strong agreement between classified maps and ground-truth data, affirming the reliability of SVM in identifying urban expansion areas. Although the Decision Tree and Minimum Distance classifiers were effective, they did not achieve the precision and accuracy of the SVM algorithm (see Table 1 and Figure 5).

Due to its superior performance, the SVM results were selected for further analysis of LULC changes. The findings reveal significant urban growth patterns between 2015 and 2020, with notable transitions from cultivated land and bare land to urban settlements. The high accuracy of the classifications, combined with the use of consistently available physical data, underscores the robustness of the proposed methodology in monitoring urban development. These results provide valuable insights into the dynamics of urban expansion over time and establish a reliable framework for future studies.

In addition to classifying the changes in LULC, this study also aimed to predict areas of future urban growth potential using a multilayer perceptron model (MLP). The MLP was configured with two hidden layers (14 and 8 nodes, respectively) and trained in more than 1,000 iterations using the LULC map from 2015, as well as six criteria identified through the Analytical Network Process (ANP) as independent variables. The binary layer of built-up areas derived from the 2020 LULC map served as the dependent variable.

To evaluate the quality of MLP predictions, built-up areas from 2024 were used for comparison. These areas were extracted from high-resolution Google Earth imagery, allowing a direct evaluation of the model's predictions against the actual urban growth observed four years after the LULC map used in training. The comparison revealed that urban growth patterns align closely with the model predictions, demonstrating its reliability. A quantitative assessment showed an 87% overlap between the predicted and actual built-up areas, further underscoring the model's accuracy.

Despite its strong performance, the model exhibited some limitations. A detailed analysis of misclassified pixels revealed that areas with mixed land uses or rapidly changing conditions presented challenges for the MLP. These findings emphasize

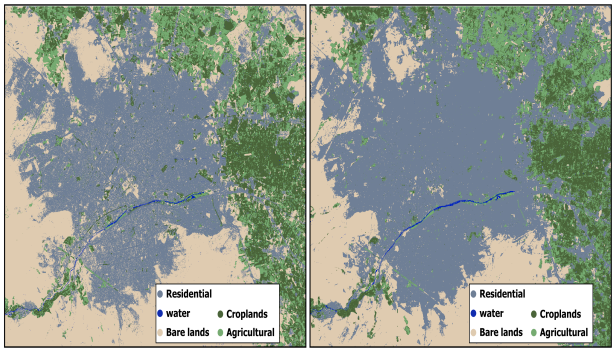

Figure 5. Land Use and Land Cover Maps for 2015 (left) and 2020 (right): Highlighting distinctive urban areas classified through high-accuracy SVM classification.

the importance of high-quality input data and the potential need for additional criteria to further improve the predictions.

The predictive results of the MLP model, visualized in Figure 6, effectively demonstrate its ability to predict urban growth. The model's integration of physical criteria provides a robust framework for monitoring and anticipating urban expansion, with potential applications in urban planning and management.

The predicted areas of urban growth from the MLP closely aligned with actual observed changes in LULC, reinforcing the model's predictive power. This suggests that the model effectively captured the complex interactions between physical factors and urban development, offering valuable insights into how these factors shape the city's growth patterns.

Moreover, the results of this study, based on SVM, ANP, and MLP, present a comprehensive understanding of Urmia's urban landscape. The LULC maps from 2015 and 2020 provided a detailed depiction of land-use dynamics, while the MLP model identified zones prone to future physical expansion. This integrative approach underscores the importance of using multi-criteria decision-making and machine learning for urban planning, with 51.97 km² of available land offering a critical resource for future development in Urmia.

Overall, this study demonstrates the effectiveness of combining machine learning algorithms, multi-criteria decision systems, and remote sensing techniques in urban studies. The SVM technique showed strong performance in LULC classification, and the ANP-MLP combination highlighted critical factors driving urban expansion, ultimately offering valuable insights for urban planners and policymakers.

5. Discussion & Conclusions

Future urban expansion will likely cluster near existing urban zones and road networks, highlighting the influence of proximity to infrastructure on growth patterns. The model predicts urbanization will follow road networks, similar to past development. Factors like lower elevation, gentle slopes, and vulnerable land uses, such as agricultural areas near city boundaries, further support this trend. These findings underscore the role of natural constraints, land use dynamics, and infrastructure accessibility in shaping urban growth.

The methodology developed in this study offers a valuable framework for assessing and predicting urban expansion, as demonstrated in Urmia. Integrating AI, MCDM, and GIS, provides

Table 1. Accuracy assessment of the Support Vector Machine (SVM) classification for 2015 and 2020. The table presents the number of correctly classified samples (correct), total samples (SUM), and producer's accuracy (PA) for each land cover class. The results show improvements in classification accuracy, particularly in the Bare lands and Residential classes in both years. PA is calculated by dividing the number of correctly predicted samples for each class by the total number of samples used to evaluate the accuracy of that class. (See equation 3)

Year	Classes	Water	Croplands	Agricultural	Residential	Bare lands	SUM
2015	Correct	38	199	167	200	293	897
	SUM	55	226	217	216	287	1001
	PA	69.09	88.05	76.95	92.59	95.47	
2020	Correct	43	106	162	271	175	757
	SUM	55	143	201	294	185	878
	PA	78.18	74.13	80.60	92.18	89.19	

robust insights applicable to diverse urban contexts. SVM analysis revealed that the 2020 built-up area covered 82.32 km², aligning with Omrani et al.'s findings (Omrani, 2019). The study identified 134.29 km² of potential urban growth areas, with 51.97 km² available for future development. These results equip planners and policymakers with a strategic foundation for sustainable and well-managed urban expansion.

The combination of SVM, ANP, and MLP techniques demonstrated high accuracy in both land use and land cover (LULC) mapping and urban growth predictions. This highlights the effectiveness of using machine learning and MCDM tools to address the complexities of urban expansion. However, while the methodology appears generalizable, its performance in different geographical and socio-economic contexts remains unproven. This limitation suggests a need for further validation to ensure broader applicability and reliability.

Additionally, the ANP method's reliance on pairwise comparisons and subjective judgments to derive criteria weights introduces potential bias, which could affect the robustness of the model. Urban expansion is driven not only by physical factors but also by complex socio-economic dynamics, which were not fully considered in this study. Future research should aim to integrate socio-economic variables alongside physical factors to better capture the multifaceted nature of urbanization processes.

This study underscores the importance of key physical factors, such as geology and proximity to roads, in shaping urban growth. While these factors are critical, refining the methodology to include socio-economic drivers and tailoring it to specific local contexts could enhance its utility. Moreover, the success of combining SVM, ANP, and MLP techniques in this study highlights the potential of machine learning and MCDM tools to address urban growth challenges effectively.

Looking ahead, the application of deep learning models and advanced AI techniques could further enhance predictive accuracy. Neural networks, for example, hold promise for forecasting urban growth in cities with development patterns similar to Urmia. Future research could explore these advanced approaches to improve model precision and adaptability.

The results of this study highlighted the importance of data-driven decision-making in urban planning. With 51.97 km² identified as available for future development, policymakers in Urmia can use these findings to implement sustainable land use strategies that minimize environmental degradation while maximizing infrastructural efficiency. The integration of AI-driven urban analysis can support proactive policy measures, ensuring controlled and well-planned expansion in rapidly growing cities.

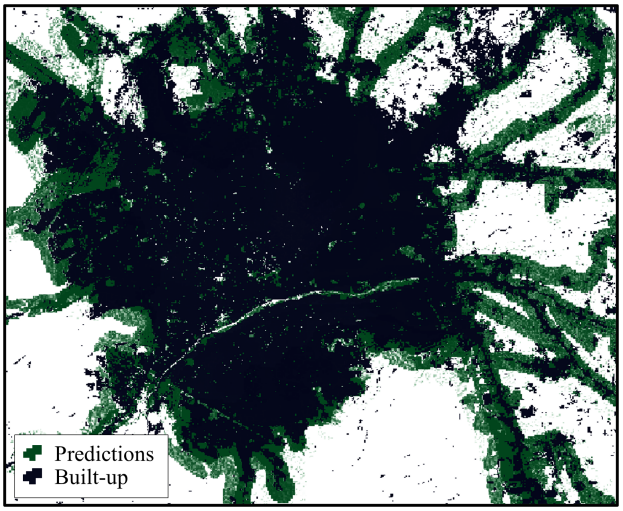

Figure 6. The predicted future urban expansion (green areas) is overlaid on the current built-up areas (black areas) derived from the 2024 Google Earth imagery. The green regions highlight areas identified by the MLP model as likely to transition into built-up zones in the future.

In conclusion, this study provides a comprehensive toolset for urban planners to proactively address the challenges of rapid urbanization. While there are areas for improvement, such as addressing biases in ANP and incorporating socio-economic drivers, the methodology offers a strong foundation for sustainable urban planning. By expanding the scope of this approach to diverse urban contexts, researchers and practitioners can develop more effective strategies for managing future urban development in harmony with environmental and infrastructural capacities.

References

Al-Fugara, A., Alshabeeb, A. R., Alshawabkeh, Y., Al-Amoush, H., Al-Adamat, R., 2018. Simulation and prediction of urban spatial expansion in highly vibrant cities using the sleuth model: A case study of Amman metropolitan, Jordan. *Theoretical and Empirical Researches in Urban Management*, 13, 37-56.

Alizadeh, M., Ngah, I., Hashim, M., Pradhan, B., Pour, A. B., 2018. A hybrid analytic network process and artificial neural network (ANP-ANN) model for urban earthquake vulnerability assessment. *Remote Sensing*, 10(6), 975.

Alizadeh Pirbasti, M., Dizbadi, Mehran, H. F. S., Davoodabadi Farahani, M., Boloori, S., 2021. Forest fire risk assessment using remote sensing techniques (study area: Golestan forest). *The 2st International Conference on GIScience: Basis Interdisciplinary, Ferdowsi University Of Mashhad , Iran*.

Amani, M., Mahdavi, S., Afshar, M., Brisco, B., Huang, W., Mohammad Javad Mirzadeh, S., White, L., Banks, S., Montgomery, J., Hopkinson, C., 2019. Canadian Wetland Inventory using Google Earth Engine: The First Map and Preliminary Results. *Remote Sensing*, 11(7).

Aziz, A., Ahmad, I., Mayo, S., Hameed, R., Nadeem, O., 2015. Urbanization and its impacts on founded areas of big cities in Pakistan: Case studies of" Ichra" and" Sanda" areas in Lahore. *University of Engineering and Technology Taxila. Technical Journal*, 20(1), 71.

Buddhiraju, K. M., Rizvi, I. A., 2010. Comparison of CBF, ANN and SVM classifiers for object based classification of high resolution satellite images. *2010 International Geoscience and Remote Sensing Symposium*, 40-43.

Cao, W., Zhou, Y., Li, R., Li, X., Zhang, H., 2021. Monitoring long-term annual urban expansion (1986–2017) in the largest archipelago of China. *Science of The Total Environment*, 776, 146015.

Castanho, R. A., Loures, L., Lousada, S., Gómez, J. M., Cabezas, J., 2022. Uncontrolled Urban Growth in Western Balkans Territories after the Communist Collapse—a Review from the Spatial Planning Perspective. *Journal of Urban Development and Management*, 1, 76-86.

Chen, C., Yan, J., Wang, L., Liang, D., Zhang, W., 2021. Classification of Urban Functional Areas From Remote Sensing Images and Time-Series User Behavior Data. *IEEE Journal of Selected Topics in Applied Earth Observations and Remote Sensing*, 14, 1207-1221.

Eastman, J., 2012. IDRISI Selva Manual. *Clark Labs, Clark University*.

Feizizadeh, B., Omarzadeh, D., Ronagh, Z., Sharifi, A., Blaschke, T., Lakes, T., 2021. A scenario-based approach for urban water management in the context of the COVID-19 pandemic and a case study for the Tabriz metropolitan area Iran. *Science of The Total Environment*, 790, 148272.

Gorelick, N., Hancher, M., Dixon, M., Ilyushchenko, S., Thau, D., Moore, R., 2017. Google Earth Engine: Planetary-scale geospatial analysis for everyone. *Remote Sensing of Environment*, 202, 18-27.

Hird, J. N., DeLancey, E. R., McDermid, G. J., Kariyeva, J., 2017. Google Earth Engine, Open-Access Satellite Data, and Machine Learning in Support of Large-Area Probabilistic Wetland Mapping. *Remote Sensing*, 9(12).

Jamali, A., Robati, M., Nikoomaram, H., Farsad, F., Aghamohammadi, H., 2023. Urban resilience assessment using hybrid MCDM model based on DEMATEL-ANP method (DANP). *Journal of the Indian Society of Remote Sensing*, 51(4), 893–915.

Khatami, R., Mountrakis, G., Stehman, S. V., 2016. A meta-analysis of remote sensing research on supervised pixel-based land-cover image classification processes: General guidelines for practitioners and future research. *Remote Sensing of Environment*, 177, 89-100.

Kodaka, A., Leelawat, N., Tang, J., Onda, Y., Kohtake, N., 2021. Government COVID-19 Responses and Subsequent Influences on NO 2 Variation in Ayutthaya, Thailand. *2021 Second International Symposium on Instrumentation*, 1–4.

LeCun, Y., Bengio, Y., Hinton, G., 2015. Deep Learning. *Nature*, 521, 436-44.

Li, H., Wan, W., Fang, Y., Zhu, S., Chen, X., Liu, B., Hong, Y., 2019. A Google Earth Engine-enabled software for efficiently generating high-quality user-ready Landsat mosaic images. *Environmental Modelling Software*, 112, 16-22.

Liang, S., 2008. Recent advances in land remote sensing: an overview. *Advances in Land Remote Sensing: System, Modeling, Inversion and Application*, 1–6.

M, A., Ahmed, S., N, H., 2023. Land use and land cover classification using machine learning algorithms in google earth engine. *Earth Science Informatics*, 16, 1-17.

Malik, N., Asmi, F., Ali, P., Rahman, M. M., 2017. Major Factors Leading Rapid Urbanization in China and Pakistan: A Comparative Study. *Journal of Social Science Studies*, 5, 148.

Mangi, M. Y., Yue, Z., Kalwar, S., Ali Lashari, Z., 2020. Comparative Analysis of Urban Development Trends of Beijing and Karachi Metropolitan Areas. *Sustainability*, 12(2).

Omarzadeh, D., Afraz, M., Akbari, M., Eftekhari, M., Noghani, Z., 2020. EVALUATION OF CHANGES IN THE FOREST ENVIRONMENT IN GUILLEN PROVINCE USING A COMBINATION OF REMOTE SENSING DATA. *Malaysian Forester*, 84, 65-83.

Omkar, S., Kumar, M. M., Mudigere, D., Muley, D., 2007. Urban Satellite Image Classification using Biologically Inspired Techniques. 1767-1772.

Omrani, M., M. M. . N. H., 2019. Spatio-temporal assessment of the spatial form of Urmia city with an emphasis on urban density indices. *Urban Planning Geography Research*, 24(3), 629–653.

Ozturk, D., 2015. Urban growth simulation of Atakum (Samsun, Turkey) using cellular automata-Markov chain and multilayer perceptron-Markov chain models. *Remote Sensing*, 7(5), 5918–5950.

Raj, S. S. A., Nair, M. S., Subrahmanyam, G. R. K. S., 2017. Satellite Image Resolution Enhancement Using Nonsubsampled Contourlet Transform and Clustering on Subbands. *Journal of the Indian Society of Remote Sensing*, 45(6).

Razavi, B. S., 2014. Predicting the trend of land use changes using artificial neural network and markov chain model (case study: Kermanshah City). *Research Journal of Environmental and Earth Sciences*, 6(4), 215–226.

Rodriguez-Galiano, V., Ghimire, B., Rogan, J., Chica, M., Rigol-Sanchez, J., 2012. An assessment of the effectiveness of a random forest classifier for land-cover classification. *ISPRS Journal of Photogrammetry and Remote Sensing*, 67, 93–104.

rostaei, s., hakimi, h., alizadeh, s., 2020. Study of Space Equity of Quantitative and qualitative indicators of housing in urban areas (Case study:Urmia city). *Human Geography Research*, 52(3), 1009-1029.

Saaty, T. L., 1996. Decision making with dependence and feedback : the analytic network process : the organization and prioritization of complexity. https://api.semanticscholar.org/CorpusID:60116026.

Sivasubramaniyan, T., RajaPerumal, R., 2024. Identifying land use land cover dynamics using machine learning method and GIS approach in Karaivetti, Tamil Nadu. *Journal of Autonomous Intelligence*, 7.

Tadono, T., Nagai, H., Ishida, H., Oda, F., Naito, S., Minakawa, K., Iwamoto, H., 2016. Generation of the 30 M-mesh global digital surface model by ALOS PRISM. *The international archives of the photogrammetry, remote sensing and spatial information sciences*, 41, 157–162.

Waske, B., Fauvel, M., Benediktsson, J., Chanussot, J., 2009. Machine Learning Techniques in Remote Sensing Data Analysis. *Kernel Methods for Remote Sensing Data Analysis*, 1 - 24.

Wingate, V. R., Phinn, S. R., Kuhn, N., Bloemertz, L., Dhanjal-Adams, K. L., 2016. Mapping Decadal Land Cover Changes in the Woodlands of North Eastern Namibia from 1975 to 2014 Using the Landsat Satellite Archived Data. *Remote Sensing*, 8(8).

Zurqani, H. A., Post, C. J., Mikhailova, E. A., Allen, J. S., 2019. Mapping Urbanization Trends in a Forested Landscape Using Google Earth Engine. *Remote Sensing in Earth Systems Sciences*, 4.